

1 **Size-Differentiated Chemical Composition of Re-Suspended Soil**
2 **Dust from the Desert Southwest United States**

3
4 **Nabin Upadhyay^{2,+}, Andrea L. Clements^{3,4++}, Matthew P. Fraser^{3,4}, Michael**
5 **Sundblom⁵⁺⁺⁺, Paul Solomon⁶, Pierre Herckes^{2*1}**

6
7 ²*Department of Chemistry and Biochemistry, Arizona State University, Tempe, AZ 85287*

8 ³*Department of Civil and Environmental Engineering, Rice University, Houston, TX 77005*

9 ⁴*School of Sustainable Engineering and the Built Environment, Arizona State University, Tempe,*
10 *AZ 85287*

11 ⁵*Pinal County Air Quality Control District, Florence, AZ 85232*

12 ⁶*US EPA Office of Research and Development, Las Vegas, NV 89119*

13 ⁺*Current Address: Global Water Sustainability Center, Qatar Science & Technology Park, PO*
14 *Box 24750, Doha, QATAR*

15 ⁺⁺*Current Address: Department of Atmospheric Science, Colorado State University, Fort*
16 *Collins, CO 80525*

17 ⁺⁺⁺*Current Address: Arizona Department of Environmental Quality, Phoenix, AZ 85007*
18

¹ *Corresponding Author: Pierre Herckes, Tel. (480) 965-4497, Fax. (480) 965-2747, email.

pierre.herckes@asu.edu

19 **ABSTRACT**

20 As part of the Desert Southwest Coarse Particulate Matter Study which characterized the
21 composition of fine and coarse particulate matter in Pinal County, AZ during 2010-2011, several
22 source samples were collected from several different soil types to assist in source apportionment
23 analysis of the study results. Soil types included native desert soils, agricultural soils (crop
24 farming), dirt-road material adjacent to agricultural areas, paved road dusts, dirt road material
25 from within and adjacent to a cattle feedlot, and material from an active cattle feedlot. Following
26 laboratory resuspension of the soil, size-segregated PM_{2.5} and PM₁₀ fractions for each source
27 type were collected on filters and characterized for mass, ions, OC, EC, and trace elements.
28 While there are unique chemical composition of soils in this region (e.g., high As and Sb) that
29 reiterate the importance of using local source profiles (e.g., native soils) as compared to Upper
30 Continental Crust or soil profiles from other regions in receptor modeling studies, the study also
31 provides new insights into the impact of land-use modification on source emission profiles.
32 Specifically, high OC and PO₄⁻³ are found in material representative of local cattle feedlot
33 activities while elevated Cu, Sb and Zn are found from sources impacted by motor vehicle
34 traffic. Results of the study indicate that the local native soil composition is only slightly
35 modified by agricultural activities and this study provides the chemical composition of both
36 native soil and agricultural for source apportionment studies in the Desert Southwest.

37

38

39 **KEY WORDS:** Cattle Feedlots, Dirt Road Dust, Paved Road Dust, Agricultural Soils,
40 Source Characterization

41

42

43 **1. INTRODUCTION**

44

45 Entrainment of crustal material can be a major source of ambient particulate matter (PM)
46 pollution. On a local scale, large fugitive dust sources can contribute to high pollution events of
47 both fine (PM_{2.5}, particles with aerodynamic diameter (AD) < 2.5 μm) and coarse (PM_c or PM_{10-2.5},
48 particles in the size range between 2.5 and 10 μm AD) particles. Understanding sources of
49 these particles is important as both size ranges have been associated with adverse health effects
50 (Pralhad et al., 1999; Ramanathan et al., 2001; Harrison et al., 2004; Solomon et al., 2011).

51 Identifying and quantifying the sources of PM is an essential step in developing
52 emissions control strategies designed to reduce levels of air pollutants to below those specified in
53 the US National Ambient Air Quality Standards (NAAQS) (40 CFR 50, 2006) which sets a limit
54 at an annual mean concentration of 12 μg/m³ PM_{2.5} averaged over a 3 year time frame (or a 35
55 μg/m³ limit at the 98% percentile averaged over 3 years) and a limit at 150 μg/m³ for PM₁₀
56 which is not to be exceeded more than once per year on average over a 3 year time frame.
57 Identifying and quantifying sources is often achieved through observational studies linking
58 emission sources to measured ambient concentrations using receptor models or other statistical
59 tools (Hopke, 1991; Hopke, 2003; Solomon and Hopke, 2008; Watson et al., 2008). In most
60 cases, a detailed knowledge of source composition is needed. Most studies that seek to quantify
61 the contribution of crustal material are limited to a small number of source samples. To improve
62 contribution estimates from different routes of crustal material entrainment to ambient PM
63 concentrations using source attribution approaches, it is essential to understand the chemical
64 composition of different source materials. On a local scale, the extent of crustal material

65 entrainment strongly depends on soil type, land-use pattern, and wind speed (Holcombe et al.,
66 1997; Macpherson et al., 2008).

67 The influence of various dust sources can be isolated only by specific chemical markers
68 unique to different source materials, and information on local soil composition is particularly
69 important in areas where crustal material is a substantial contributor to airborne PM. One such
70 region is the arid desert of the southwestern United States (US), including Arizona. A recent
71 study estimated that resuspended dust accounts for as much as 20% of PM_{2.5} and 76% of PM_c in
72 the southwestern US (Malm et al., 2007). Pinal County, in central Arizona, is an area that
73 frequently exceeds the PM₁₀ NAAQS (U.S. EPA AirData, 2012). Many of these exceedances are
74 attributed to resuspended dust from agricultural activities, unpaved and paved roads,
75 construction, and desert lands. In addition, agricultural activities, like soil preparation, cattle
76 farming, and movement of cattle in feedlots might contribute substantially to local high PM
77 events. However, lack of comprehensive chemical characterization of various soil types in
78 different particle size ranges within the study area limits the understanding of potential sources
79 and the relative impact of each on the PM concentrations on a local scale.

80 This study presents the detailed chemical composition of local soils in central Arizona
81 with the goal of contrasting chemical composition of material from different land uses to aid in
82 source apportionment. Source profiles are developed for several soil types including soils that are
83 potentially representative of the southwestern US. The specific objectives of the study are to
84 characterize the chemical composition of soils associated with possible sources that contribute to
85 ambient PM_{2.5} and PM₁₀ concentrations, and to determine if there are specific chemical markers
86 to differentiate among various soil types. Size-segregated soil samples (PM_{2.5} and PM₁₀)
87 collected from twelve different locations representing 5 different land use types in Pinal County

88 were analyzed for detailed chemical composition allowing source profiles to be developed and
89 compared to the composition of UCC and to undisturbed native desert soils.

90

91 **2. EXPERIMENTAL**

92

93 **Soil Sampling**

94 A summary of the sampling locations, local soil types, and soil classifications for this
95 study is provided in Table 1. All soil samples were collected in Pinal County, AZ (USA) in the
96 vicinity of three different air quality monitoring sites, including Pinal County Housing (PCH),
97 Casa Grande (CG), and Cowtown (COW). A detailed description of the monitoring sites and
98 local PM composition can be found elsewhere (Clements et al., 2012), with only a brief summary
99 of the sites given here. PCH is a rural site located in immediate proximity to native (undisturbed)
100 desert land with agricultural fields within a mile in all directions. Soil samples near PCH were
101 collected from native desert soils (denoted native - NAT) from immediate proximity to the air
102 quality monitoring site (less than 40 meters distant), from the edge and within the cropping area
103 of an agricultural field to the north of the monitoring site (denoted agricultural - AGR), and from
104 the edge of a dirt road used to access the agricultural fields in the area (denoted dirt road
105 agricultural – DRA). The CG site is located in the small urban area of Casa Grande, AZ.
106 Potential source samples in the vicinity of CG were collected at the edge of a local roadway
107 representing paved road dust material (denoted paved road dust – PAV). COW is a rural
108 monitoring location with unique local emission sources, which include a grain processing plant
109 to the southwest of the air quality monitoring site and a confined cattle feedlot to the south of the
110 air quality monitoring site. Samples near this location included soils from the native desert in the

111 immediate vicinity of the monitoring site (less than 40 meters distant) (NAT), within the active
112 and fallowed agricultural fields to the east, north, and west of the site (AGR), the median
113 between the monitoring site and a local two-lane highway (NAT), and the edge of the dirt roads
114 near the cattle feedlot (denoted dirt road feedlot – DRF). Material representative of the soil found
115 within the cattle feedlots was also collected (denoted feedlot – FDL).

116 Using this set of 11 fixed sampling sites, soil samples were collected during spring, fall,
117 and winter seasons with additional samples collected during unique events (e.g., a cotton field
118 during cotton defoliation). In total, 35 soil samples were collected. All samples were obtained
119 from the top 15 mm of the surface using a trowel, or by a hand broom from paved roadway
120 surface, and placed into pre-baked glass jars for storage and transport (Hagen, 2004). Figure 1
121 shows the location of the fixed ambient monitoring locations and the nearby locations where soil
122 samples were collected.

123

124 **Soil Resuspension**

125 All soil samples were resuspended in the laboratory to simulate the process of windblown
126 dust entrainment and to obtain samples representative of the composition of PM_{2.5} and PM₁₀ size
127 fractionated aerosols for subsequent chemical analysis. Soil source samples were prepared for
128 resuspension by heating to 110°C for 24 hr (similar to Carvacho et. al. (Carvacho et al., 2004))
129 and gently compressed to break up large soil aggregates (clumps larger than the size of a dime);
130 care was taken to not grind the material to avoid mechanical abrasion of small particles. Once
131 prepared, samples were introduced into a clean flask and HEPA-filtered air was passed over the
132 sample to resuspend small particles. The resuspended particles were passed through a size-
133 selective cyclone (URG Corporation) and collected on downstream filter media (similar to

134 Carcacho et. al. (Carvacho et al., 2004)). The operating flow rates were determined based on the
135 cyclone design – 28 L/min for PM₁₀ sampling and 42 L/min for PM_{2.5} sampling. These flow rates
136 were well within the range of flow rates used in other soil resuspension experiments (Carvacho
137 et al., 2004; Etyemezian et al., 2007). Three filters, including one Teflon and two quartz-fiber
138 filters were collected in parallel for each reentrainment experiment. A minimum target of ~8 mg
139 of resuspended material was established to provide enough material for the planned detailed
140 chemical analysis. Sampling was periodically stopped so the Teflon filter could be removed to
141 determine the amount of collected material; the filter was reinstalled and sampling continued
142 until the target mass was achieved or exceeded. On average, 20 mg of soil was collected on each
143 filter. Depending on the crustal material studied, a varying period of time was required to reach
144 target mass levels: road dust, for instance, required approximately 20 minutes to collect the
145 minimum mass while some agricultural soils required upwards of 4 hours.

146

147 **Soil Chemical Analysis**

148 Re-suspended soil samples were analyzed chemically in a manner similar to ambient PM
149 samples; details including procedures, analytical precision, and quality control measures are
150 reported elsewhere (Clements et al., 2012). Gravimetric mass was determined by the difference
151 between the pre- and post-collection weights of the Teflon filter. Sample weights were measured
152 under controlled temperature ($22\text{ }^{\circ}\text{C} < T < 24\text{ }^{\circ}\text{C}$) and humidity conditions ($45\% < \text{RH} < 55\%$) to
153 minimize water-uptake (U.S. EPA, 2006).

154 Following gravimetric analysis, the Teflon filter was microwave-digested using an acid
155 mixture according to the method of Upadhyay, et al. (Upadhyay et al., 2009; Clements et al.,
156 2012). The extract was then analyzed for 63 elements by high-resolution inductively coupled

157 plasma mass spectrometry (ICP-MS) (ThermoFinnigan ELEMENT 2) using an internal indium
158 standard. Elements quantified included, but were not limited to, Al, As, Ba, Ca, Cd, Co, Cr, Cu,
159 Fe, K, Mg, Mn, Mo, Na, Ni, P, Pb, Rb, Sb, Se, Sn, Ti, U, V, Zn. All elements reported were
160 measured well above method detection limits (MDLs). The elements in PM_{2.5} and PM₁₀ soil
161 samples are one order (As, Cd, Cr, Na, Ni, and Sb) to five orders (Pb) of magnitudes higher than
162 the MDLs. The instrument was calibrated using a multi-element standard (SPEX Certiprep Inc.)
163 and two National Institute of Standards and Technology standard reference materials (San
164 Joaquin Soil SRM 2709 and Urban Dust SRM 1649) were also measured for quality control and
165 element concentrations were within 100 ± 20% of the certified values.

166 Water-soluble ions were measured from a set of two 1.5-cm² punches that were removed
167 from one of the two quartz-fiber filters and extracted in 7.5 mL ultrapure water for 15 minutes in
168 an ultrasonic bath at room temperature. Extracts were filtered using a syringe filter (Millex GP
169 0.22 µm pore size PES membrane filter) and then analyzed for cations (sodium, potassium,
170 ammonium, calcium, and magnesium) and anions (chloride, nitrate, phosphate, and sulfate) by
171 ion chromatograph (Dionex IC20, Dionex Corporation) equipped with CG12A and AS12A
172 analytical columns.

173 Bulk organic carbon (OC), elemental carbon (EC), and total carbon (TC) concentrations
174 were analyzed by thermal-optical transmittance (TOT) (Birch and Cary, 1996) using a slightly
175 modified thermal protocol as described in Clements et al. (Clements et al., 2012).

176

177 **3. RESULTS AND DISCUSSION**

178

179 **Chemical composition**

180 Bulk chemical concentrations, including organic carbon and major mineral elements such
181 as Al, Fe, K, etc., showed consistency within each sample type across each season, so samples
182 were aggregated into groups according to land use type. Tables 2 and 3 present the average
183 chemically speciated source profiles for PM_{2.5} and PM₁₀ for each land use type, respectively.
184 Standard deviations (SD) represent the pooled average of the land use samples for each category.
185 Method detection limits (MDLs) for chemical species were calculated based on 3 x SD of filter
186 blanks and the notation BDL refers to concentrations below the MDL. Analytical uncertainties
187 are given in Tables S1 (for PM_{2.5}) and S2 (for PM₁₀) for reference. The chemical profiles for
188 each category were similar for both PM_{2.5} and PM₁₀ with the contribution for most chemical
189 species within the range of the variability as measured by the SD. For all categories, Al, Ca, Fe,
190 K, and Mg are the most abundant elemental species observed (weight percent $\geq 1\%$), which is
191 consistent with the known bulk composition of crustal material. Organic carbon (OC) is also a
192 substantial component ($> 1\%$ of PM mass) for all categories in both size fractions.

193 The relative abundance of OC is between 2 and 17 times higher for feedlot (FDL)
194 samples compared to the other soil types. Sulfate and phosphate are both found in the greatest
195 abundance in FDL samples. The elevated abundance of these particular species is consistent with
196 nature of the cattle feeding operations and possibly is influenced by the chemical composition of
197 the feed used in the feeding operation.

198 The relative abundance of OC in paved road (PAV) samples is about 2-6 times higher
199 than in the other source categories excluding FDL. The relative abundance of elemental carbon
200 (EC) is more than an order of magnitude higher in PAV than in samples from other categories,
201 including native soils (NAT), dirt roads near agricultural site (DRA), and agricultural soils
202 (AGR), where the EC values are below detection limits. Several anthropogenic elements

203 including copper, lead, and zinc are higher by factors of 3 -10 in PAV relative to other source
204 categories; the presence and abundance of these elements suggest origin from vehicular sources.
205 These results are consistent with high concentrations of these elements in ambient PM_{2.5}
206 collected from a parking garage in Tempe, Arizona (Majestic et al., 2009). Lough et al (Lough et
207 al., 2005) suggest that the dominance of Ba, Cu, Pb, and Zn are associated with both tail-pipe
208 emissions and mechanical abrasion of vehicle brakes and lead weights used to balance tires.

209 The relative abundance of the chemical components measured in NAT, AGR, and DRA
210 samples are, in general, similar to each other even though samples were collected from different
211 land use regions. Exceptions to this observation include sulfate and sodium ion, which are about
212 4 – 10 times higher in DRA compared to NAT and AGR samples. Although there is variability in
213 composition among the source categories, ammonium, nitrate, and chloride ions also show a
214 pattern of being an order of magnitude higher in DRA compared to NAT and AGR samples. All
215 5 of these species are components of agricultural wastes and fertilizers and have been reported as
216 markers for active agricultural farms (Cao et al., 2008). Elevated relative abundances of these
217 ions found in DRA samples, rather than AGR samples, are likely due to overspray of fertilizers,
218 the active mixing of soil by moving vehicles, deposition of windblown dust onto the road from
219 the adjacent agricultural fields, runoff from fields, and/or the lack of regular irrigation that occurs
220 on AGR during growing season. Depressed abundances of these ions in the NAT and AGR
221 samples may be the result of uptake by native or agricultural plants.

222 The relative abundances of calcium, nitrate, and sulfate were higher in samples from dirt
223 roads near the feedlot (DRF) than the other source categories; both PM_{2.5} and PM₁₀ size fractions
224 showed this enrichment. Calcium and sulfate species may be a result of the application of
225 calcium lignosulfonate, a by-product of wood processes, which has been used as both a dust

226 suppressant (Ouyang et al., 2006) and as an animal feed binder (Kaliyan and Vance Morey,
227 2009). Concentrations of these species, in excess of that found in the natural soils, may be
228 distinct fingerprints for the use calcium lignosulfonate as a soil stabilizer or animal feed binder.

229 As previously noted, the relative abundances of Al, Ca, Fe, K, and Mg are high in all
230 source types in both the PM_{2.5} and PM₁₀ size fractions. However, the lowest relative abundance
231 of Al and Fe are found in feedlot samples due to the higher fraction of organic material in this
232 source category (Tables 2 and 3). Of particular interest in the FDL samples, the concentrations of
233 PO₄³⁻ and P are considerably higher than observed in other source categories. PO₄³⁻ and P
234 abundances were 2.8% and 1.4% in PM_{2.5} and 3.9% and 1.3% in PM₁₀, respectively. Higher
235 concentrations of nutrient-related species (e.g., K, K⁺, Na⁺, Mg²⁺, Cl⁻, Ca²⁺, Ca, and SO₄²⁻) are
236 also found in FDL samples. These results indicate that PO₄³⁻ and K⁺ may be distinct markers for
237 entrainment of material from FDL sources, although soluble K (K⁺) also is a marker for wood
238 combustion (Calloway et al., 1989; Khalil and Rasmussen, 2003). These results are consistent
239 with feedlot profiles reported in a previous study (Chow et al., 2003). The correlation of cations
240 to anions can be used to corroborate possible ion pairing: Cl⁻ in FDL is fairly well-correlated
241 with Na⁺, K⁺, and NH₄⁺ ($R^2 \geq 0.82$), while Mg²⁺ and PO₄³⁻ as well as K⁺ and SO₄²⁻ are also well-
242 correlated ($R^2 \geq 0.90$) indicating that these correlated components may be associated as salts.

243 **Total versus soluble fractions of elements**

244 Samples were extracted in water to determine the water-soluble ionic concentration
245 which was compared to the total element concentration determined by acid digestion to
246 determine a water-soluble fraction. The water-soluble fraction of selected elements in PM_{2.5} and
247 PM₁₀ is shown in Figure 2 for each source type. The mole fraction of P in PO₄³⁻ (soluble P) was
248 used to calculate the water-soluble fraction of phosphorus. Results show enhanced solubility for

249 Na, K, and P in FDL samples and Ca in DRF samples relative to the other source types. Greater
250 than half of the Na is in the form of soluble salts in both size fractions for DRA, DRF, and FDL
251 and for AGR in PM₁₀. The other components were fairly insoluble showing greater amounts of
252 insoluble material compared to soluble material. All components were measured to be more
253 soluble in PM₁₀ than PM_{2.5}. The higher solubility of the selected elements in PM₁₀ rather than in
254 PM_{2.5} suggests that the soluble ions associated with soil fertility are predominantly present in the
255 coarse particle size range.

256 Figure 2 shows DRF samples are distinct in terms of soluble Ca with about 70% and 80%
257 solubility in PM_{2.5} and PM₁₀, respectively. This further supports the application of calcium
258 lignosulfonate as a soil stabilizer (Ouyang et al., 2006) or animal feed binder (Kaliyan and Vance
259 Morey, 2009) as it readily disassociates into ionic species in water. In other soil types, soluble
260 Ca ranged between 10% to 20% in both size fractions. Higher solubility of Ca in conjunction
261 with high SO₄²⁻ appears to be a good source signature for DRF samples. Samples from the
262 feedlot showed that all (ratio ≈ 1) of the Na, K, and P found in these samples were soluble.
263 Overall, results suggest that the soils from cattle feedlots are chemically different and that there
264 are markers species, especially K⁺ and PO₄³⁻, that can be used to discriminate this soil type from
265 the natural soil sources, although care must be taken as soluble K (K⁺) is also a marker for wood
266 combustion (Calloway et al., 1989).

267

268 **Reconstructed Mass Balance**

269 A mass balance relating gravimetrically determined mass to measured species can verify
270 that major components have been accounted for by the targeted analytes. The mass balance
271 summary and major components are shown in Figure 3. The *organic matter* (OM) component

272 was determined as 1.4 x OC (Turpin and Lim, 2001). The *crustal* component was based on the
273 reconstructed soil mass determined by the IMPROVE (Interagency Monitoring of Protected
274 Visual Environment) approach (Eldred, 2003; DeBell, 2006).

275

$$276 \quad \text{Crustal} = 2.20 * \text{Al} + 2.49 * \text{Si} + 1.63 * \text{Ca} + 2.42 * \text{Fe} + 1.94 * \text{Ti} \quad (1)$$

277

278 The carbonate and water components that are sometimes included in the crustal calculation were
279 not directly measured in the study and are excluded from the calculation of crustal material.

280 Since Si was not analyzed by ICP-MS, its mass in the sample was estimated based on the
281 average ratio of Si/Al = 3.5. This value was estimated based on the average Si/Al ratios of 3.8
282 observed in the average composition of upper continental crust (UCC) (Taylor and McLennan,
283 1995); 3.0 observed road dust or agricultural soil in the Imperial Valley, California, USA
284 (Watson and Chow, 2001); and 3.5 observed in road dust in an urban area of Texas, USA (Chow
285 et al., 2004). The *phosphate* and *sulfate* components are pure components containing just the
286 ionic species themselves. The *non-crustal K* component was determined by difference between
287 the measured K and the calculated crustal K where crustal K was determined as 0.6 x Fe (Malm
288 et al., 2004). The *trace element* component was determined as the sum of all other trace metals
289 not included in the crustal equation with no correction factors applied and ionic species not
290 accounted for as pure components. The reconstructed mass balance showed that these
291 components, on average, account for 102 ± 8% of resuspended crustal mass across all sites, with
292 crustal as the single dominant component of PM_{2.5} and PM₁₀.

293 Crustal material is the dominant contributor to all source types in both size fractions
294 (Figure 3). It accounts for 63% and 81% of FDL and DRF, respectively and from 94-100%

295 across the other source types in the PM_{2.5} size range. For PM₁₀, crustal material accounted for
296 44% of FDL and between 78-91% of the other source types. These results are consistent with
297 findings that report soil elements are the major components of fine and coarse PM in Phoenix
298 (Katrinak et al., 1995; Tolocka et al., 2001; Lewis et al., 2003). OM in PM_{2.5} ranged from less
299 than 5% in NAT, AGR, and DRA to 10% in PAV, to a maximum of 37% in FDL. SO₄²⁻ was a
300 major contributor to the composition of DRF accounting for approximately 21% of the PM₁₀
301 mass. The smaller crustal fraction in FDL samples is offset by the higher fraction of OM, SO₄²⁻,
302 and non-soil K, with these three components accounting for 49% PM₁₀ mass. This is consistent
303 with cattle feeding and farm operations where manure adds a significantly amount of organic
304 material to native soils. Overall, the mass closure agrees to within 20%. These results indicate
305 that human activities, such as motor vehicle traffic and cattle farming activities, can greatly
306 modify the chemical characteristics of entrained crustal material from sources impacted by these
307 activities.

308

309 **Enrichment Factors**

310 Enrichment factors (EFs) compare the abundance of a given component in a sample (e.g.,
311 soil or ambient sample) relative to that same component in a reference material to isolate unique
312 features to potentially use as tracer species. In this case, the average trace element composition
313 of each source type is compared to an average reference crustal material and EFs greater than 1
314 show enrichment of the given element, likely due to a local source. The EF of an element (X) is
315 most commonly calculated relative to the published average composition of UCC (Taylor and
316 McLennan, 1995) using Al or Fe as the reference element (R) (Dodd et al., 1991) where EF =
317 $[X/R]_{\text{sample}} / [X/R]_{\text{UCC}}$. The EFs of selected elements relative to UCC using Al as the reference

318 element are reported in Figure 4. While similar trends are observed for both PM_{2.5} and PM₁₀,
319 several unique features are observed. Numerous elements including As, Ca, Cu, Ni, P, Pb, Sb,
320 and Zn are enriched (EF>5) in most source types with As, Cu, P, Sb, and Zn enriched by an
321 order of magnitude or more compared to UCC. All samples, including NAT and AGR soils are
322 enriched in As and Sb suggesting regional influence from local emission sources and/or pollutants
323 from long-range transport. Vehicular emissions are important sources of Cu, Pb, and Zn
324 (Seinfeld and Pandis, 1997; Maykut et al., 2003; Utsunomiya et al., 2004; Solomon and Hopke,
325 2008) and could account for enrichment in PAV samples and others potentially influenced by
326 vehicle and train traffic. Consistent with the mass abundance in the soil profiles, P has the
327 highest EF of 75 ± 50 in PM_{2.5} and 76 ± 52 in PM₁₀ in the FDL samples, indicating the
328 significant alteration of the local soil caused by the cattle feeding operations.

329 To more realistically account for local geochemical conditions to isolate if sources are
330 enriched by local sources, EFs were determined based on a comparison to the composition of
331 unaltered desert soils (NAT) obtained during this study (Figure 5). Al was again used as the
332 reference element. The native land in the sampling area is not routinely cultivated or fertilized
333 and was not part of a roadway, so this material is less impacted by agricultural chemicals and
334 vehicular emissions. For most elements, there were very minimal alterations compared to EFs
335 based on UCC composition. However, the enrichment of As and Sb in all soil types when EFs
336 are determined relative to UCC is not observed when the EFs are determined relative to local
337 native desert soil. This indicated the ubiquitous nature of these elements in crustal material
338 common to this region. This observation is supported by reports of elevated As levels in soil and
339 ground water in the southwestern US (Focazio et al., 2000). No elements are enriched in AGR
340 relative to NAT, suggesting little anthropogenic influence of trace elements through farming

341 practices. Progressively, a larger number of elements are enriched in DRA, PAV, DRF, and FDL
342 samples. Vehicular and industrial emissions appear to impact the elemental components (such as
343 Pb, Cu, Sb, Sn, and Zn) of paved road dust samples and P enrichment is significant in FDL
344 samples.

345

346 **4. CONCLUSIONS**

347

348 Samples collected from crustal material representing different land uses in Pinal County,
349 AZ were resuspended in the laboratory, including material representing native desert (NAT),
350 agricultural crop farming (AGR), dirt roads adjacent to agricultural areas (DRA), paved roads
351 (PAV), dirt road within and adjacent to a cattle feedlot (DRF), and a cattle feedlot (FDL).

352 Following resuspension of the material in the laboratory, size-segregated PM_{2.5} and PM₁₀
353 fractions for each source type were collected on filters and characterized for mass, ions, OC, EC,
354 and trace elements. Results showed that the chemical abundances for the majority of species are
355 similar between source category between PM_{2.5} and PM₁₀ samples. Elements common to crustal
356 sources (Al, Ca, Fe, and Mg), K, and OC are abundant in all soil types (mass percent by weight
357 $\geq 1\%$), Ca and Ca⁺², and SO₄²⁻ are most abundant in DRF, and OC and PO₄³⁻ are most abundant
358 in FDL. Data suggest that soluble phosphate is a possible unique marker for entrainment of
359 crustal material from cattle feedlots. Calcium and sulfate present in some dirt road samples may
360 be related to calcium lignosulfonate used as a dust suppressant or animal feed binder.

361 Vehicular movement and wind likely help mix agricultural soil with dirt roads within the
362 vicinity of agricultural fields (DRA). This mixing and overspray of fertilizers likely results in an
363 increase in the relative abundance of NH₄⁺, SO₄²⁻, NO₃⁻, Cl⁻, and Na, which are an order of

364 magnitude more abundant in DRA when compared to NAT and AGR samples. Decreased
365 abundances of these elements in the fallow and crop lands are suggestive of removal from the
366 soils by plant uptake. Fugitive dust emissions from the undisturbed agricultural soil may
367 therefore contain lower concentrations of these species than the dust released during the land
368 preparation. The abundance of Cu, Pb, and Zn are an order of magnitude higher in PAV
369 compared to other source types, consistent with motor vehicle sources. Mass balance analysis
370 showed that the crustal component comprises most of the particle mass in both PM_{2.5} and PM₁₀.

371 The unique chemical composition of soils in this region (e.g., high As and Sb) shows the
372 importance of using local soil profiles (e.g., native soils) as compared to UCC or soil profiles
373 from other regions in receptor modeling studies. Failure to use a region specific source soil
374 profile in an apportionment study may lead to inappropriate apportionment of crustal particles to
375 other sources. In this case, elevated arsenic concentrations in the native soil could have been
376 mischaracterized as anthropogenic rather than natural which might have lead to apportionment of
377 the aerosol to a smelting source not present or contributing to PM concentrations in this airshed.
378 Source material composition also indicates the impact of local sources modifying the soil
379 composition from NAT. For example, high OC and PO₄³⁻ were associated with the cattle feedlot
380 and Cu, Sb, and Zn were associated with paved roads.

381

382 **5. ACKNOWLEDGEMENTS**

383

384 The authors thank Dr. Yuling Jia for her assistance with sample re-suspensions. Funding
385 for this work was provided through a Regional Applied Research Effort (RARE), Region 9 and
386 the Pinal County Air Quality Control District. The United States Environmental Protection

387 Agency through its Office of Research and Development partially funded and collaborated in the
388 research described here under assistance agreement 83404901 to Arizona State University. It has
389 been subjected to Agency review and approved for publication.

390

391 **6. REFERENCES**

392

393 40 CFR 50. 2006. National Ambient Air Quality Standards for Particulate Matter; Final Rule:
394 Federal Register. Vol. 71, No. 200.

395 Birch, M. E. and R. A. Cary. 1996. Elemental carbon-based method for monitoring occupational
396 exposures to particulate diesel exhaust. *Aer. Sci. & Tech.* 25(3): 221-241.

397 Calloway, C. P., S. Li, et al. 1989. A Refinement of Potassium Tracer Method for Residential
398 Wood Smoke. *Atmos. Env.* 23(1): 67-69. doi:10.1016/0004-6981(89)90098-x.

399 Cao, J. J., J. C. Chow, et al. 2008. Size-differentiated source profiles for fugitive dust in the
400 Chinese Loess Plateau. *Atmos. Env.* 42(10): 2261-2275.

401 doi:10.1016/j.atmosenv.2007.12.041.

402 Carvacho, O. F., L. L. Ashbaugh, et al. 2004. Measurement of PM_{2.5} emission potential from
403 soil using the UC Davis resuspension test chamber. *Geomorph.* 59(1-4): 75-80.

404 doi:10.1016/j.geomorph.2003.09.007.

405 Chow, J. C., J. G. Watson, et al. 2003. Similarities and differences in PM₁₀ chemical source
406 profiles for geological dust from the San Joaquin Valley, California. *Atmos. Env.* 37(9-

407 10): 1317-1340. doi:10.1016/s1352-2310(02)01021-x.

408 Chow, J. C., J. G. Watson, et al. 2004. Source profiles for industrial, mobile, and area sources in
409 the Big Bend Regional Aerosol Visibility and Observational study. *Chemosphere* 54(2):
410 185-208.

411 Clements, A. L., M. P. Fraser, et al. 2012. Chemical characterization of coarse particulate matter
412 in the desert Southwest - Pinal County Arizona, USA. *Atmos. Env.* submitted.

413 DeBell, L. J. 2006. Spatial and seasonal patterns and temporal variability of haze and its
414 constituents in the United States: Report IV: Cooperative Institute for Research in the
415 Atmosphere.
416 [http://vista.cira.colostate.edu/IMPROVE/Publications/Reports/2006/PDF/IMPROVE_Re](http://vista.cira.colostate.edu/IMPROVE/Publications/Reports/2006/PDF/IMPROVE_Report_IV.pdf)
417 [port_IV.pdf](http://vista.cira.colostate.edu/IMPROVE/Publications/Reports/2006/PDF/IMPROVE_Report_IV.pdf) (accessed 25 November 2012).

418 Dodd, J. A., J. M. Ondov, et al. 1991. Multimodal Size Spectra Of Submicrometer Particles
419 Bearing Various Elements In Rural Air. *Env. Sci. & Tech.* 25(5): 890-903.

420 Eldred, B. 2003. Evaluation of the equation for soil composite: Internal memo to IMPROVE
421 staff.
422 http://vista.cira.colostate.edu/IMPROVE/Publications/GrayLit/023_SoilEquation/Soil_Eq
423 [_Evaluation.pdf](http://vista.cira.colostate.edu/IMPROVE/Publications/GrayLit/023_SoilEquation/Soil_Eq_Evaluation.pdf) (accessed 24 November 2012).

424 Etyemezian, V., G. Nikolich, et al. 2007. The Portable In Situ Wind Erosion Laboratory (PI-
425 SWERL): A new method to measure PM10 potential for windblown dust properties and
426 emissions. *Atmos. Env.* 41(18): 3789-3796. doi:10.1016/j.atmosenv.2007.01.018.

427 Focazio, M. J., A. H. Welch, et al. 2000. A Retrospective Analysis on the Occurrence of Arsenic
428 in Ground-Water Resources of the United States and Limitations in Drinking-Water-
429 Supply Characterizations. *U.S. Geological Survey; Water-Resources Investigations*
430 *Report 99-4279; available at <http://pubs.usgs.gov/wri/wri994279/>*

431 Hagen, L. J. 2004. Fine particulates (PM10 and PM2.5) generated by breakage of mobile
432 aggregates during simulated wind erosion. *Transactions of the ASAE*, 47(1): 107-112.

433 Harrison, R. M., D. J. T. Smith, et al. 2004. What is responsible for the carcinogenicity of
434 PM2.5? *Occ. & Env. Med.* 61(10): 799-805.

435 Holcombe, T. L., T. Ley, et al. 1997. Effects of prior precipitation and source area characteristics
436 on threshold wind velocities for blowing dust episodes, Sonoran Desert 1948-78. *J. of*
437 *App. Met.* 36(9): 1160-1175.

438 Hopke, P. K. (1991). Receptor modeling for air quality management. Amsterdam, The
439 Netherlands, Elsevier. pp.

440 Hopke, P. K. 2003. Recent developments in receptor modeling. *J. of Chemometrics* 17(5): 255-
441 265. doi:10.1002/cem.796.

442 Kaliyan, N. and R. Vance Morey. 2009. Factors affecting strength and durability of densified
443 biomass products. *Biomass and Bioenergy* 33(3): 337-359.

444 Katrinak, K. A., J. R. Anderson, et al. 1995. Individual Particle Types In The Aerosol Of
445 Phoenix, Arizona. *Env. Sci. & Tech.* 29(2): 321-329.

446 Khalil, M. A. K. and R. A. Rasmussen. 2003. Tracers of wood smoke. *Atmos. Env.* 37(9-10):
447 1211-1222. doi:10.1016/s1352-2310(02)01014-2.

448 Lewis, C. W., G. A. Norris, et al. 2003. Source apportionment of phoenix PM2.5 aerosol with the
449 Unmix receptor model. *J. Air & Waste Manag. Ass.* 53(3): 325-338.

450 Lough, G. C., J. J. Schauer, et al. 2005. Emissions of metals associated with motor vehicle
451 roadways. *Env. Sci. & Tech.* 39(3): 826-836. doi:10.1021/es048715f.

- 452 Macpherson, T., W. G. Nickling, et al. 2008. Dust emissions from undisturbed and disturbed
453 supply-limited desert surfaces. *J. of Geophy. Res.-Earth Surface* 113(F2).
454 doi:F02s0410.1029/2007jf000800.
- 455 Majestic, B. J., A. D. Anbar, et al. 2009. Elemental and iron isotopic composition of aerosols
456 collected in a parking structure. *Sci. Of The Tot. Env.* 407(18): 5104-5109.
- 457 Malm, W. C., K. Gebhart, et al. 2004. Pacific Northwest Regional Visibility Experiment Using
458 Natural Tracers - Chapter 4: Aerosol Sample Analysis.
459 <http://vista.cira.colostate.edu/improve/Studies/PREVENT/Reports/FinalReport/CHAP4.p>
460 [re.pdf](http://vista.cira.colostate.edu/improve/Studies/PREVENT/Reports/FinalReport/CHAP4.p) (accessed 11 December 2012).
- 461 Malm, W. C., M. L. Pitchford, et al. 2007. Coarse particle speciation at selected locations in the
462 rural continental United States. *Atmos. Env.* 41(10): 2225-2239.
463 doi:10.1016/j.atmosenv.2006.10.077.
- 464 Maykut, N. N., J. Lewtas, et al. 2003. Source apportionment of PM_{2.5} at an urban IMPROVE
465 site in Seattle, Washington. *Env. Sci. & Tech.* 37(22): 5135-5142.
- 466 Ouyang, X., X. Qiu, et al. 2006. Physicochemical characterization of calcium lignosulfonate--A
467 potentially useful water reducer. *Colloids & Surfaces A: Physicochem. & Eng. Aspects*
468 282-283: 489-497.
- 469 Prahalad, A. K., J. M. Soukup, et al. 1999. Ambient air particles: Effects on cellular oxidant
470 radical generation in relation to particulate elemental chemistry. *Tox. & App. Pharma.*
471 158(2): 81-91.
- 472 Ramanathan, V., P. J. Crutzen, et al. 2001. Atmosphere - Aerosols, climate, and the hydrological
473 cycle. *Sci.* 294(5549): 2119-2124.

474 Seinfeld, J. H. and S. N. Pandis (1997). Atmospheric Chemistry and Physics: From Air Pollution
475 to Climate Change, Wiley-Interscience. pp.

476 Solomon, P. A., M. Costantini, et al. 2011. Air Pollution and Health: Bridging the Gap from
477 Sources to Health Outcomes: Conference Summary. *Air Qual., Atmos. & Health* 5(1): 9-
478 62. doi:10.1007/s11869-011-0161-4.

479 Solomon, P. A. and P. K. Hopke. 2008. A special issue of JA&WMA supporting key scientific
480 and policy- and health-relevant findings from EPA's particulate matter supersites
481 program and related studies: An integration and synthesis of results. *J. of the Air & Waste*
482 *Manag. Ass.* 58(2): 137-139. doi:10.3155/1047-3289.58.2.137.

483 Taylor, S. R. and S. M. McLennan. 1995. The Geochemical Evolution Of The Continental-Crust.
484 *Rev. Of Geophysics* 33(2): 241-265.

485 Tolocka, M. P., P. A. Solomon, et al. 2001. East versus West in the US: Chemical characteristics
486 of PM_{2.5} during the winter of 1999. *Aer. Sci. & Tech.* 34(1): 88-96.
487 doi:10.1080/02786820118957.

488 Turpin, B. J. and H. J. Lim. 2001. Species contributions to PM_{2.5} mass concentrations:
489 Revisiting common assumptions for estimating organic mass. *Aer. Sci. & Tech.* 35(1):
490 602-610.

491 U.S. EPA. 2006. 40 CFR 50: National Ambient Air Quality Standards for Particulate Matter
492 (Final Rule). <http://www.epa.gov/ttn/amtic/40cfr50.html> (accessed).

493 U.S. EPA AirData, 2012. Access to Air Pollution Data. <http://www.epa.gov/airdata/> (accessed
494 July 2011]).

495 Upadhyay, N., B. J. Majestic, et al. 2009. Evaluation of polyurethane foam, polypropylene,
496 quartz fiber, and cellulose substrates for multi-element analysis of atmospheric

497 particulate matter by ICP-MS. *Anal. & Bioanal. Chem.* 394(1): 255-266.
498 doi:10.1007/s00216-009-2671-6.

499 Utsunomiya, S., K. A. Jensen, et al. 2004. Direct identification of trace metals in fine and
500 ultrafine particles in the Detroit urban atmosphere. *Env. Sci. & Tech.* 38(8): 2289-2297.

501 Watson, J. G., L. W. A. Chen, et al. 2008. Source apportionment: Findings from the US
502 Supersites program. *J. of the Air & Waste Manag. Ass.* 58(2): 265-288.
503 doi:10.3155/1047-3289.58.2.265.

504 Watson, J. G. and J. C. Chow. 2001. Source characterization of major emission sources in the
505 Imperial and Mexicali Valleys along the US/Mexico border. *Sci. Of The Total Env.*
506 276(1-3): 33-47.

507
508

509 **List of Table Titles**

510 **Table 1.** Source Sampling Details

511 **Table 2.** Average (\pm SD) of source profile chemical compositions (weight percent by mass) of
512 resuspended PM_{2.5} material

513 **Table 3.** Average (\pm SD) of source profile chemical compositions (weight percent by mass) of
514 resuspended PM₁₀ material

515
516 **Table S1.** Average analytical uncertainty of source profile chemical components (weight percent by mass
517 of resuspended PM_{2.5} material)

518
519 **Table S2.** Average analytical uncertainty of source profile chemical components (weight percent by mass
520 of resuspended PM₁₀ material)

521

522

523

Table 1. Source Sampling Details

Site Number	Season	Closest Monitor	Sampling Location	Soil type	Sample Category	Classification
1	Spring	PCH	20 Meters SW of Monitoring Site	Fine Sandy Loam	Native	NAT
1	Fall	PCH	20 Meters SW of Monitoring Site	Fine Sandy Loam	Native	NAT
1	Winter	PCH	20 Meters SW of Monitoring Site	Fine Sandy Loam	Native	NAT
2	Spring	PCH	40 Meters SW of Monitoring Site	Fine Sandy Loam	Native	NAT
2	Fall	PCH	40 Meters SW of Monitoring Site	Fine Sandy Loam	Native	NAT
2	Winter	PCH	40 Meters SW of Monitoring Site	Fine Sandy Loam	Native	NAT
3	Spring	COW	20 Meters SW of Monitoring Site	Clay Loam	Native	NAT
3	Fall	COW	20 Meters SW of Monitoring Site	Clay Loam	Native	NAT
3	Winter	COW	20 Meters SW of Monitoring Site	Clay Loam	Native	NAT
4	Winter	COW	Median between Site and Highway	Clay Loam	Native	NAT
5	Spring	COW	East Alfalfa Field	Clay Loam	Agricultural	AGR
5	Fall	COW	East Alfalfa Field	Clay Loam	Agricultural	AGR
5	Winter	COW	East Alfalfa Field	Clay Loam	Agricultural	AGR
6	Spring	COW	West Alfalfa Field	Clay Loam	Agricultural	AGR
6	Fall	COW	West Alfalfa Field	Clay Loam	Agricultural	AGR
7	Spring	PCH	Winter Wheat Field - Edge	Fine Sandy Loam	Agricultural	AGR
7	Spring	PCH	Winter Wheat Field - Center	Fine Sandy Loam	Agricultural	AGR
7	Fall	PCH	Winter Wheat Field - Center	Fine Sandy Loam	Agricultural	AGR
7	Winter	PCH	Winter Wheat Field - Center - Cut	Fine Sandy Loam	Agricultural	AGR
8	Fall	PCH	Defoliated Cotton Field	Fine Sandy Loam	Agricultural	AGR
8	Winter	PCH	Fallow Cotton Field	Fine Sandy Loam	Agricultural	AGR
9	Spring	PCH	Dirt Road Dust - South Edge	Fine Sandy Loam	Dirt Road - Ag	DRA
9	Fall	PCH	Dirt Road Dust - South Edge	Fine Sandy Loam	Dirt Road - Ag	DRA
9	Winter	PCH	Dirt Road Dust - South Edge	Fine Sandy Loam	Dirt Road - Ag	DRA
10	Spring	PCH	Dirt Road Dust - North Edge	Fine Sandy Loam	Dirt Road - Ag	DRA
10	Fall	PCH	Dirt Road Dust - North Edge	Fine Sandy Loam	Dirt Road - Ag	DRA
11	Winter	CG	Paved Road - Edge Composite	Fine Sandy Loam	Paved Road	PAV
12	Spring	COW	Dirt Road Dust - Near Feedlot	Clay Loam	Dirt Road - Feed	DRF
12	Fall	COW	Dirt Road Dust - Near Feedlot	Clay Loam	Dirt Road - Feed	DRF
13	Spring	COW	Feedlot Material	Clay Loam	Feedlot	FDL
13	Fall	COW	Feedlot Material	Clay Loam	Feedlot	FDL
13	Fall	COW	Feedlot Material	Clay Loam	Feedlot	FDL
13	Winter	COW	Feedlot Material	Clay Loam	Feedlot	FDL
14	Winter	COW	Empty Feedlot Material	Clay Loam	Empty feedlot	FDL
15	Winter	COW	Old Feedlot Surface Material	Clay Loam	Empty feedlot	FDL

PCH - Pinal County Housing; COW - Cowtown; CG - Casa Grande
 NAT - Native Soil; AGR - Agricultural Soil; PAV - Paved Road Dust; DRA - Dirt (Unpaved) Road Dust from an Agricultural Area;
 DRF - Dirt (Unpaved) Road Dust from a Cattle Feedlot Area; FDL - Soil from a Cattle Feedlot

525
526

527

Table 2. Average (\pm SD) of source profile chemical compositions (weight percent by mass) of resuspended PM_{2.5} material^a

Species	Soil Classification				
	NAT	AGR	DRA	PAV ^b	DRF
OC	1.2 \pm 0.7	3 \pm 2	1.7 \pm 0.5	7	2.8 \pm
EC	BDL	BDL	BDL	0.2	0.002 \pm
TC	1.2 \pm 0.7	3 \pm 2	1.7 \pm 0.5	7	2.8 \pm
Cl ⁻	0.02 \pm 0.03	0.04 \pm 0.03	0.2 \pm 0.2	0.08	0.5 \pm
NO ₃ ⁻	0.05 \pm 0.09	0.03 \pm 0.02	0.2 \pm 0.2	0.05	0.8 \pm
PO ₄ ³⁻	0.06 \pm 0.03	0.09 \pm 0.06	0.02 \pm 0.02	0.15	0.10 \pm

SO ₄ ²⁻	0.03 ± 0.04	0.1 ± 0.2	0.6 ± 0.2	0.2	17 ±
Na ⁺	0.09 ± 0.05	0.20 ± 0.08	0.8 ± 0.2	0.2	0.46 ±
NH ₄ ⁺	0.06 ± 0.05	0.12 ± 0.10	0.5 ± 0.5	0.02	0.2 ±
K ⁺	0.11 ± 0.03	0.14 ± 0.07	0.07 ± 0.02	0.07	0.369 ±
Mg ²⁺	0.02 ± 0.01	0.04 ± 0.02	0.02 ± 0.01	0.02	0.09 ±
Ca ²⁺	0.4 ± 0.2	0.7 ± 0.5	0.5 ± 0.2	0.6	6 ±
Al	8 ± 1	7 ± 3	7 ± 1	7	5 ±
As	0.0012 ± 0.0003	0.0014 ± 0.0003	0.0014 ± 0.0002	0.002	0.001 ±
Ba	0.054 ± 0.004	0.05 ± 0.02	0.05 ± 0.01	0.06	0.04 ±
Ca	2.2 ± 0.3	4 ± 2	6 ± 1	3	10 ±
Cd	0.0001 ± 0	0.0001 ± 0	0 ± 0	0.0002	0.00003 ±
Co	0.002 ± 0	0.002 ± 0.001	0.0016 ± 0.0002	0.002	0.0010 ±
Cr	0.005 ± 0.001	0.004 ± 0.001	0.005 ± 0.000	0.007	0.003 ±
Cs	0.0016 ± 0.0003	0.002 ± 0.001	0.0011 ± 0.0002	0.001	0.0011 ±
Cu	0.008 ± 0.002	0.010 ± 0.005	0.0049 ± 0.0004	0.03	0.007 ±
Fe	4.0 ± 0.2	3.7 ± 1.0	3.7 ± 0.4	4	2.5 ±
Ga	0.0022 ± 0.0002	0.002 ± 0.001	0.0017 ± 0.0002	0.002	0.0015 ±
K	3.6 ± 0.7	3.0 ± 0.5	3.2 ± 0.9	2	2.8 ±
Mg	1.9 ± 0.4	1.6 ± 0.5	2.1 ± 0.5	2	1.2 ±
Mn	0.15 ± 0.01	0.13 ± 0.04	0.12 ± 0.02	0.09	0.08 ±
Na	0.31 ± 0.03	0.4 ± 0.1	1.2 ± 0.2	0.6	0.56 ±
Ni	0.004 ± 0.001	0.004 ± 0.001	0.003 ± 0	0.005	0.002 ±
P	0.12 ± 0.01	0.13 ± 0.04	0.11 ± 0.01	0.2	0.26 ±
Pb	0.007 ± 0.002	0.006 ± 0.002	0.003 ± 0	0.02	0.004 ±
Rb	0.013 ± 0.002	0.011 ± 0.004	0.012 ± 0.002	0.01	0.008 ±
Sb	0.0002 ± 0.0001	0.0002 ± 0.0001	0.00015 ± 0.00001	0.001	0.0002 ±
Sr	0.019 ± 0.002	0.03 ± 0.01	0.045 ± 0.005	0.02	0.041 ±
Th	0.0017 ± 0.0003	0.002 ± 0.001	0.0015 ± 0.0003	0.002	0.0014 ±
Ti	0.30 ± 0.04	0.27 ± 0.09	0.27 ± 0.05	0.3	0.17 ±
V	0.0081 ± 0.0003	0.008 ± 0.002	0.007 ± 0.001	0.008	0.006 ±
Zn	0.020 ± 0.002	0.020 ± 0.007	0.014 ± 0.001	0.1	0.018 ±

530 ^aSD was calculated from the average of the aggregated samples from each site

531 ^bNo SD is included for PAV because only one sample was collected

532 BDL - below detection limit as defined in the text

533

534

535

536

537

538

539

540

541
 542
 543
 544
 545
 546
 547
 548

Table 3. Average (\pm SD) of source profile chemical compositions (weight percent by mass) of resuspended PM₁₀ material^a

Species	Soil Classification				
	NAT	AGR	DRA	PAV ^b	DRF
OC	1.3 \pm 0.4	2 \pm 1	2.0 \pm 0.5	8	3.9 \pm 0.4
EC	BDL	BDL	BDL	0.2	0.02 \pm 0.01
TC	1.3 \pm 0.4	2 \pm 1	2.0 \pm 0.5	8	3.9 \pm 0.4
Cl ⁻	0.02 \pm 0.02	0.01 \pm 0.01	0.2 \pm 0.2	0.11	0.3 \pm 0.03
NO ₃ ⁻	0.07 \pm 0.12	0.03 \pm 0.02	0.2 \pm 0.2	0.04	1 \pm 2
PO ₄ ³⁻	0.07 \pm 0.03	0.1 \pm 0.1	0.03 \pm 0.03	0.18	0.12 \pm 0.03
SO ₄ ²⁻	0.04 \pm 0.05	0.1 \pm 0.1	0.8 \pm 0.2	0.2	24 \pm 24
Na ⁺	0.09 \pm 0.04	0.2 \pm 0.2	0.8 \pm 0.2	0.2	0.61 \pm 0.06
NH ₄ ⁺	0.05 \pm 0.04	0.1 \pm 0.1	0.5 \pm 0.4	0.02	0.3 \pm 0.03
K ⁺	0.10 \pm 0.02	0.12 \pm 0.06	0.06 \pm 0.00	0.07	0.51 \pm 0.05
Mg ²⁺	0.02 \pm 0.01	0.03 \pm 0.02	0.011 \pm 0.004	0.02	0.09 \pm 0.01
Ca ²⁺	0.4 \pm 0.2	0.6 \pm 0.4	0.4 \pm 0.3	0.7	8 \pm 8
Al	7 \pm 1	7 \pm 1	5 \pm 2	7	5 \pm 2
As	0.0011 \pm 0.0004	0.0014 \pm 0.0003	0.0013 \pm 0.0002	0.002	0.0013 \pm 0.0003
Ba	0.049 \pm 0.007	0.044 \pm 0.007	0.046 \pm 0.003	0.06	0.04 \pm 0.01
Ca	2.2 \pm 0.5	4 \pm 3	5.8 \pm 1.0	3	9 \pm 3
Cd	0.00006 \pm 0.00002	0.00006 \pm 0.00001	0.00004 \pm 0.00001	0.0002	0.00004 \pm 0.00001
Co	0.0016 \pm 0.0001	0.0015 \pm 0.0002	0.0014 \pm 0.0001	0.001	0.0010 \pm 0.0001
Cr	0.004 \pm 0.001	0.0035 \pm 0.0005	0.0044 \pm 0.0001	0.007	0.003 \pm 0.001
Cs	0.0014 \pm 0.0003	0.0015 \pm 0.0003	0.0010 \pm 0.0002	0.001	0.0012 \pm 0.0003
Cu	0.007 \pm 0.002	0.008 \pm 0.001	0.0045 \pm 0.0004	0.03	0.006 \pm 0.001
Fe	3.7 \pm 0.4	3.3 \pm 0.5	3.4 \pm 0.2	4	2.4 \pm 0.3
Ga	0.0019 \pm 0.0002	0.0018 \pm 0.0003	0.0016 \pm 0.0001	0.002	0.0014 \pm 0.0003
K	3.2 \pm 0.8	2.9 \pm 0.6	3.0 \pm 0.6	2	2.8 \pm 0.3
Mg	1.7 \pm 0.5	1.5 \pm 0.3	1.8 \pm 0.6	1	1.1 \pm 0.1
Mn	0.13 \pm 0.02	0.11 \pm 0.02	0.11 \pm 0.01	0.09	0.07 \pm 0.01
Na	0.31 \pm 0.03	0.36 \pm 0.08	1.2 \pm 0.3	0.7	0.62 \pm 0.06
Ni	0.004 \pm 0.003	0.0029 \pm 0.0003	0.003 \pm 0	0.005	0.0022 \pm 0.0003
P	0.11 \pm 0.02	0.11 \pm 0.02	0.10 \pm 0.01	0.2	0.26 \pm 0.03
Pb	0.006 \pm 0.002	0.005 \pm 0.001	0.0032 \pm 0.0003	0.01	0.004 \pm 0.001
Rb	0.012 \pm 0.003	0.010 \pm 0.003	0.010 \pm 0.001	0.01	0.009 \pm 0.001
Sb	0.0002 \pm 0	0.0002 \pm 0.0001	0.0001 \pm 0	0.001	0.0002 \pm 0

Sr	0.018 ± 0.003	0.03 ± 0.01	0.046 ± 0.006	0.03	0.039 ± 0
Th	0.002 ± 0	0.0015 ± 0.0004	0.0012 ± 0.0004	0.002	0.001 ± 0
Ti	0.28 ± 0.05	0.24 ± 0.04	0.26 ± 0.02	0.3	0.19 ± 0
V	0.0075 ± 0.0005	0.007 ± 0.001	0.0070 ± 0.0004	0.007	0.005 ± 0
Zn	0.018 ± 0.003	0.016 ± 0.003	0.014 ± 0.003	0.1	0.018 ± 0

549 ^aSD was calculated from the average of the aggregated samples from each site

550 ^bNo SD is included for PAV because only one sample was collected

551 BDL - below detection limit as defined in the text

552

553

554

555
556

Table S1. Average analytical uncertainty of source profile chemical components (weight percent by mass of resuspended PM_{2.5} material)

Species	Soil Classification					
	NAT	AGR	DRA	PAV	DRF	FDL
OC	0.1	0.2	0.1	0.4	0.2	1.1
EC	0.0	0.03	0.02	0.03	0.02	0.08
TC	0.1	0.2	0.1	0.4	0.2	1.1
Cl ⁻	0.007	0.007	0.007	0.007	0.007	0.007
NO ₃ ⁻	0.007	0.007	0.007	0.007	0.007	0.007
PO ₄ ²⁻	0.006	0.006	0.006	0.006	0.006	0.1
SO ₄ ²⁻	0.006	0.006	0.006	0.006	6	0.1
Na ⁺	0.001	0.001	0.001	0.001	0.001	0.001
NH ₄ ⁺	0.004	0.004	0.004	0.004	0.004	0.004
K ⁺	0.005	0.005	0.005	0.005	0.005	0.005
Mg ²⁺	0.002	0.002	0.002	0.002	0.002	0.002
Ca ²⁺	0.003	0.003	0.003	0.003	0.003	0.003
Al	0.3	0.4	0.4	0.5	0.2	0.2
As	0.0003	0.0004	0.0003	0.0003	0.0002	0.0004
Ba	0.002	0.002	0.002	0.003	0.001	0.002
Ca	0.2	0.3	0.3	0.1	0.7	0.4
Cd	0.00001	0.00001	0.00001	0.00002	0.00001	0.00001
Co	0.0001	0.0002	0.0001	0.0002	0.0001	0.0002
Cr	0.0002	0.0003	0.0003	0.0003	0.0002	0.0003
Cs	0.00003	0.00005	0.00004	0.00011	0.00004	0.00005
Cu	0.0003	0.0006	0.0004	0.0005	0.0004	0.0007
Fe	0.1	0.1	0.1	0.01	0.1	0.04
Ga	0.0001	0.0002	0.0001	0.0003	0.0001	0.0002
K	0.1	0.1	0.1	0.2	0.1	0.3
Mg	0.1	0.1	0.1	0.1	0.1	0.1
Mn	0.003	0.005	0.004	0.002	0.002	0.002
Na	0.02	0.03	0.05	0.03	0.05	0.07
Ni	0.0003	0.0006	0.0004	0.0001	0.0004	0.0006
P	0.003	0.005	0.008	0.003	0.006	0.053
Pb	0.0002	0.0003	0.0002	0.0011	0.0002	0.0002
Rb	0.001	0.001	0.001	0.001	0.001	0.001
Sb	0.00001	0.00002	0.00001	0.00005	0.00001	0.00002
Sr	0.0004	0.0005	0.0012	0.0003	0.0008	0.0015
Th	0.00005	0.00006	0.00006	0.00003	0.00005	0.00003
Ti	0.006	0.012	0.007	0.008	0.005	0.008
V	0.0003	0.0005	0.0003	0.0008	0.0003	0.0003
Zn	0.001	0.001	0.001	0.008	0.001	0.006

557
558

559
560

Table S2. Average analytical uncertainty of source profile chemical components (weight percent by mass of resuspended PM₁₀ material)

Species	Soil Classification					
	NAT	AGR	DRA	PAV	DRF	FDL
OC	0.1	0.2	0.1	0.4	0.2	1.2
EC	0.0	0.03	0.02	0.04	0.02	0.07
TC	0.1	0.2	0.1	0.4	0.2	1.2
Cl ⁻	0.007	0.007	0.007	0.007	0.1	0.007
NO ₃ ⁻	0.007	0.007	0.007	0.007	0.007	0.007
PO ₄ ²⁻	0.006	0.006	0.006	0.006	0.006	0.1
SO ₄ ²⁻	0.006	0.006	0.006	0.006	8	0.1
Na ⁺	0.001	0.001	0.001	0.001	0.001	0.001
NH ₄ ⁺	0.004	0.004	0.004	0.004	0.004	0.004
K ⁺	0.005	0.005	0.005	0.005	0.005	0.005
Mg ²⁺	0.002	0.002	0.002	0.002	0.002	0.002
Ca ²⁺	0.003	0.003	0.003	0.003	0.1	0.003
Al	0.4	0.4	0.4	0.7	0.5	0.2
As	0.0003	0.0005	0.0002	0.0001	0.0002	0.0003
Ba	0.002	0.002	0.002	0.002	0.002	0.001
Ca	0.1	0.2	0.3	0.0	0.5	0.2
Cd	0.00001	0.00001	0.00001	0.00002	0.00001	0.00001
Co	0.0001	0.0002	0.0001	0.0001	0.0001	0.0002
Cr	0.0002	0.0003	0.0003	0.0005	0.0002	0.0004
Cs	0.00005	0.00006	0.00004	0.00005	0.00005	0.00004
Cu	0.0003	0.0004	0.0003	0.0002	0.0003	0.0005
Fe	0.1	0.1	0.1	0.20	0.2	0.04
Ga	0.0001	0.0002	0.0002	0.0002	0.0001	0.0001
K	0.1	0.1	0.1	0.2	0.2	0.3
Mg	0.1	0.1	0.1	0.2	0.1	0.1
Mn	0.004	0.004	0.005	0.005	0.002	0.002
Na	0.02	0.02	0.06	0.07	0.04	0.04
Ni	0.0005	0.0003	0.0003	0.0011	0.0003	0.0006
P	0.005	0.006	0.006	0.009	0.008	0.072
Pb	0.0003	0.0003	0.0001	0.0009	0.0002	0.0002
Rb	0.001	0.001	0.001	0.000	0.001	0.001
Sb	0.00001	0.00002	0.00001	0.00007	0.00001	0.00001
Sr	0.0004	0.0008	0.0012	0.0011	0.0010	0.0007
Th	0.00005	0.00006	0.00004	0.00007	0.00004	0.00005
Ti	0.010	0.010	0.015	0.016	0.005	0.006
V	0.0003	0.0003	0.0003	0.0005	0.0002	0.0003
Zn	0.001	0.001	0.001	0.002	0.001	0.002

561
562

563 **List of Figure Captions**

564 **Figure 1.** Depiction of the ambient sampling locations and the associated soil sampling locations
565 in close proximity.

566

567 **Figure 2.** Soluble fraction of selected elements in PM_{2.5} and PM₁₀ across six sampling sites. The
568 mole fraction of P in PO₄³⁻ (sol P) was used to calculate the water-soluble fraction of
569 phosphorus.

570

571 **Figure 3.** Mass balance for resuspended soil collected as PM_{2.5} and PM₁₀. Error bars represent
572 the total propagated error calculated from the standard deviation of samples within each soil type
573 for each chemical component. The definition of each category can be found under the heading
574 Reconstructed Mass Balance. The category titles are given in italics.

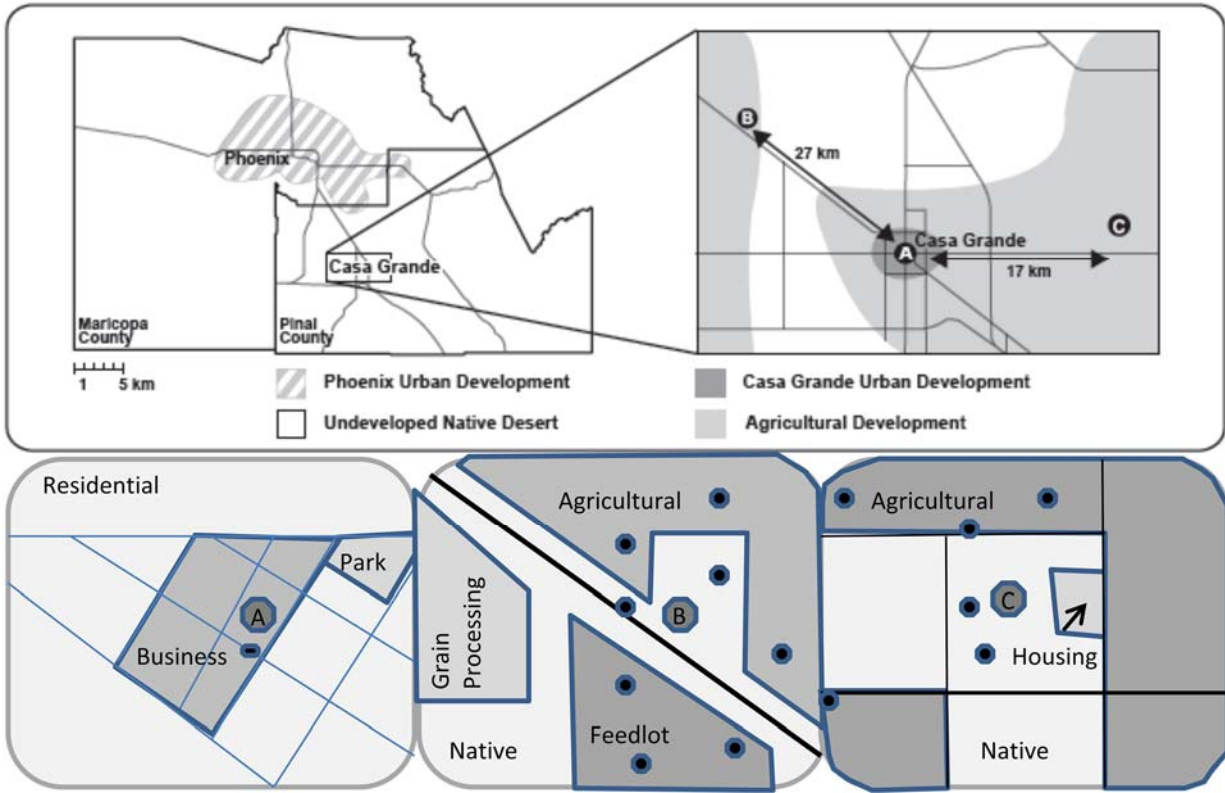
575

576 **Figure 4.** Enrichment factors for elements in PM_{2.5} and PM₁₀ resuspended soil samples relative
577 to average composition of upper continental crust. Ba, Ce, Fe, Rb, Th, Ti, V, and Y have EFs
578 between 1 and 2 and are not included in the plot. The horizontal green line denotes an EF of 1
579 while boxed numbers indicate the EFs for elements that go off-scale.

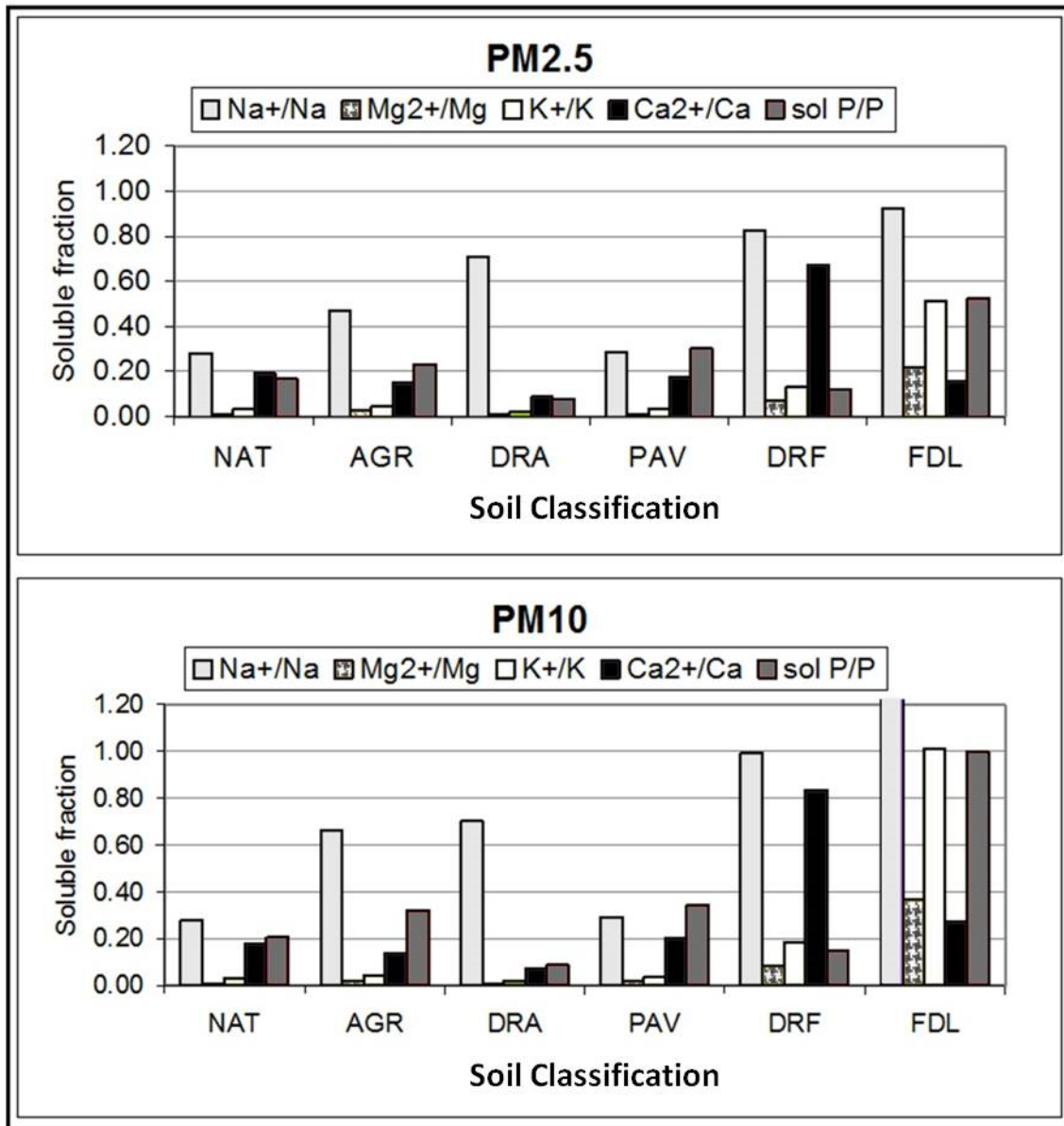
580

581 **Figure 5.** Enrichment factors for elements in PM_{2.5} and PM₁₀ resuspended soil samples relative
582 to native soil collected at PCH and COW. Ba, Ce, Fe, Rb, Th, Ti, V, and Y have EFs between 1
583 and 2 and are not included in the plot. The horizontal green line denotes an EF of 1 while boxed
584 numbers indicate the EFs for elements that go off-scale.

585

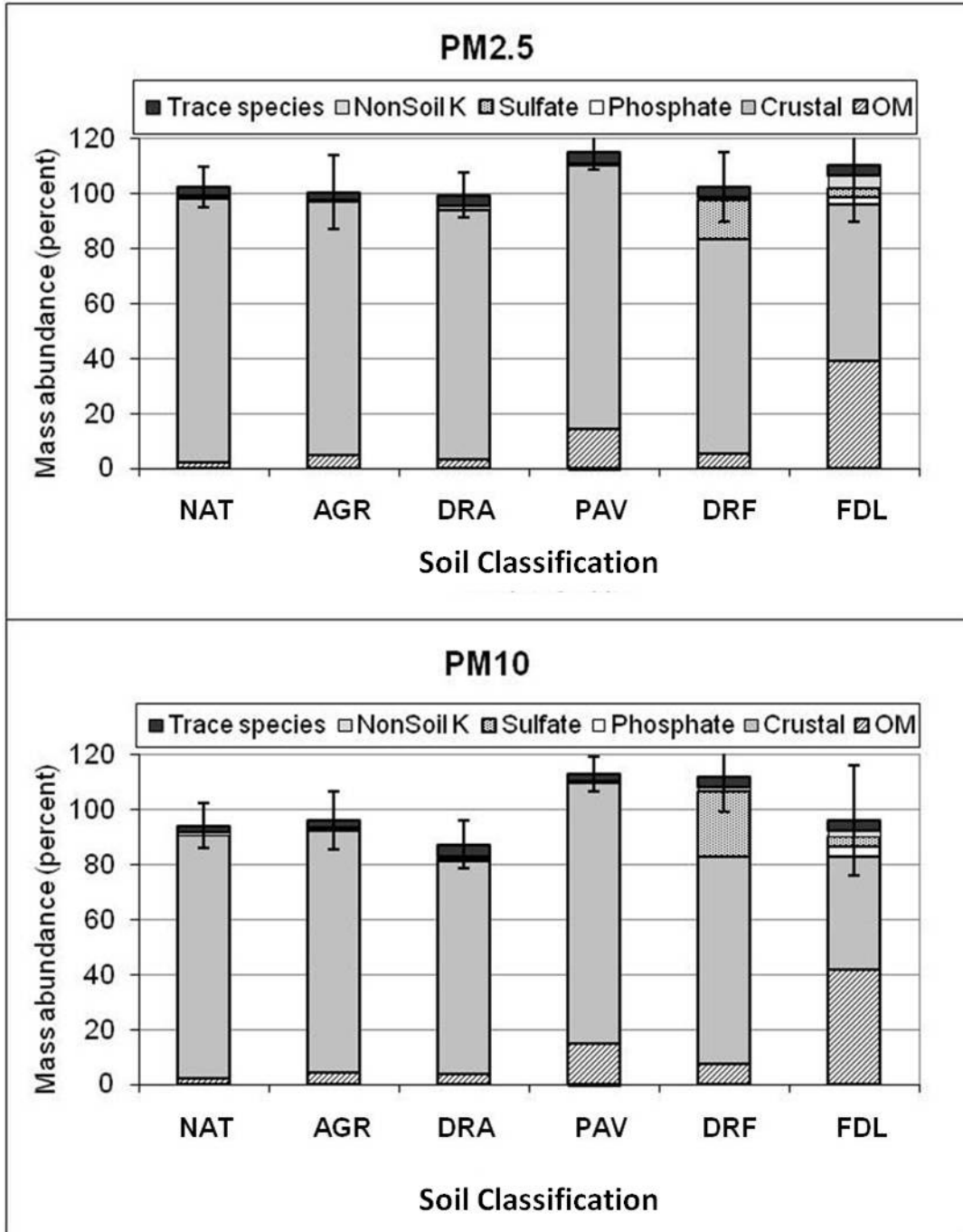


586
 587 **Figure 1**
 588

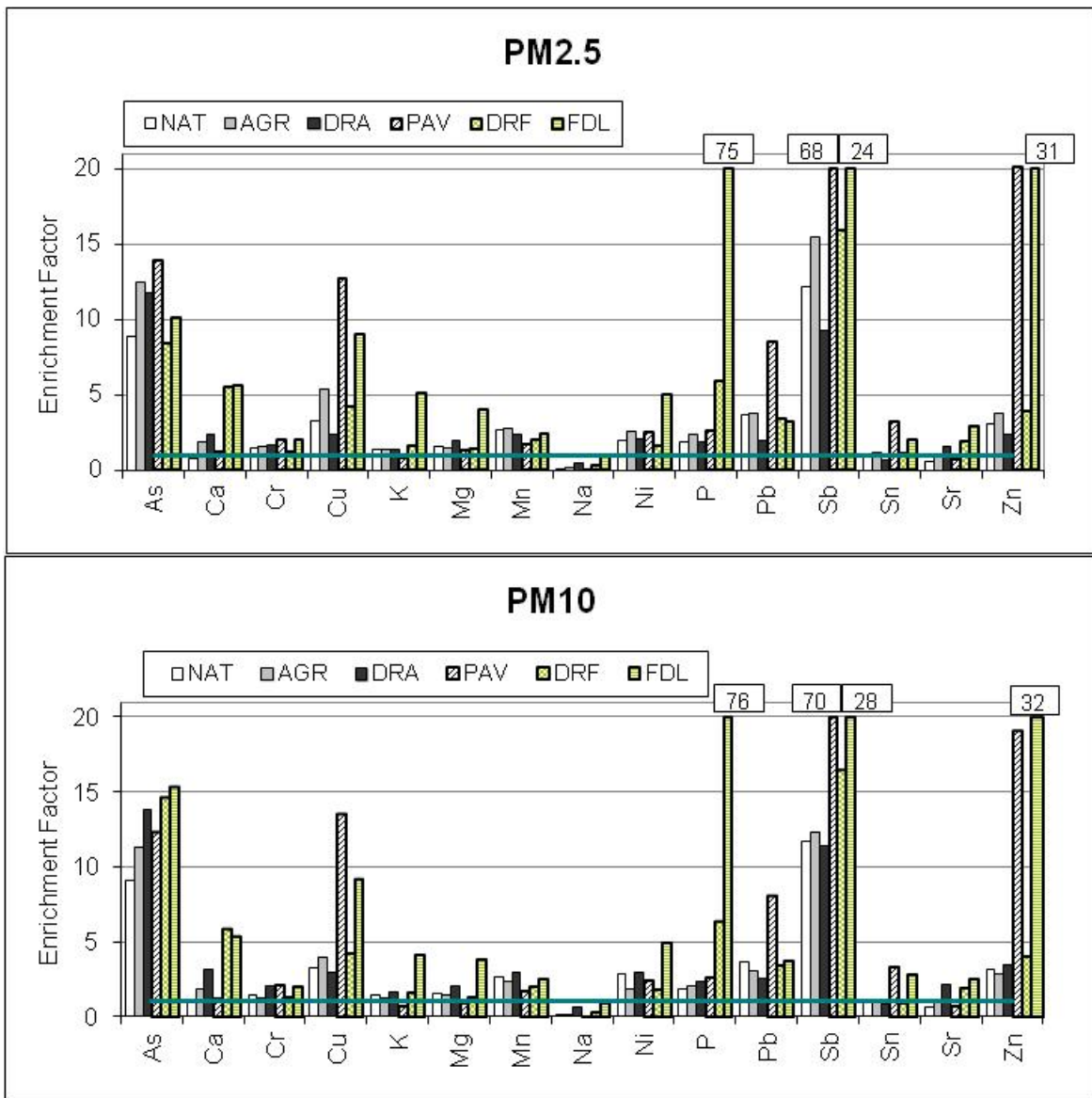


589
590

Figure 2

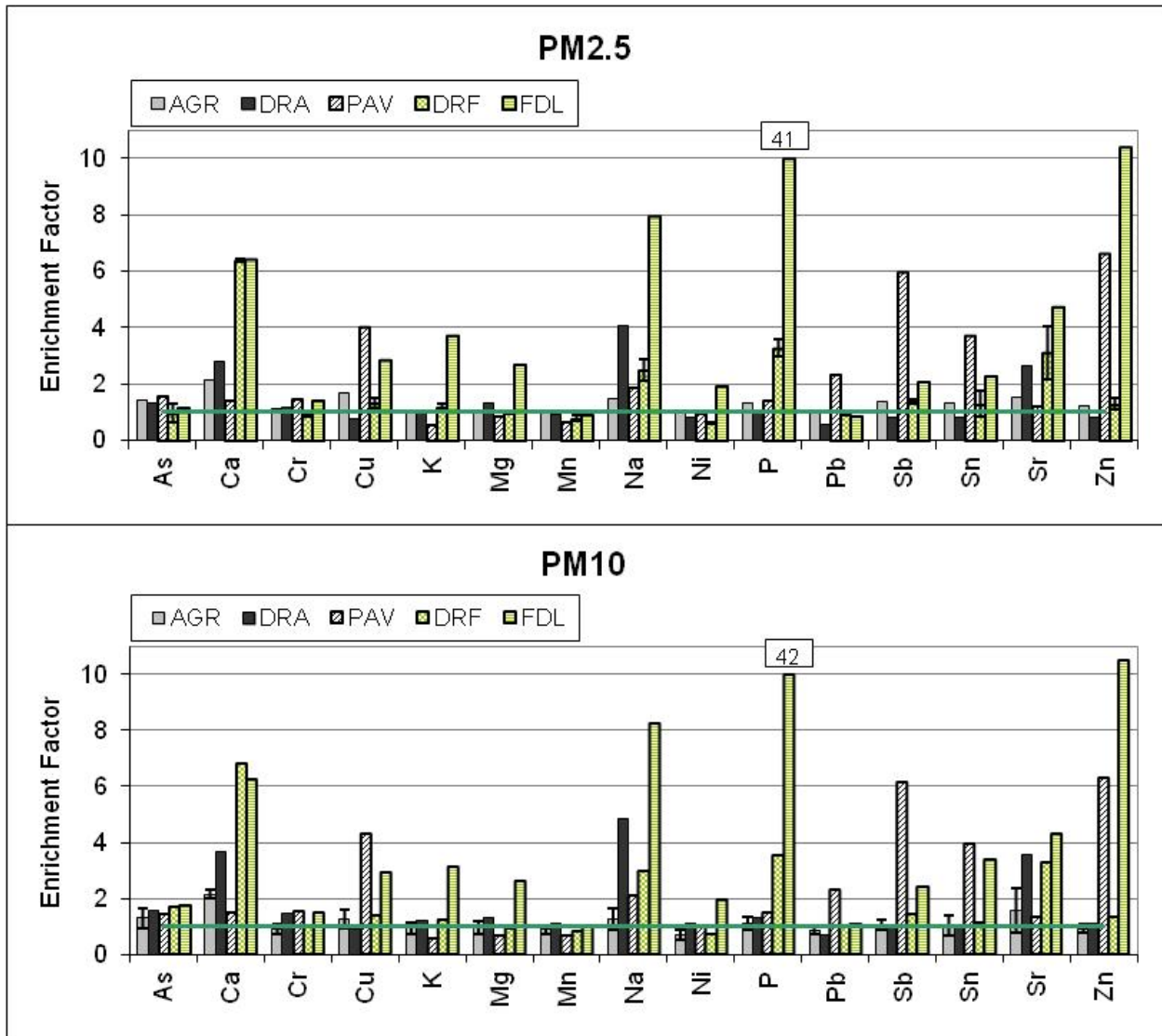


591
 592 **Figure 3**
 593



594
595

Figure 4



596
597

Figure 5